Flexible Electromagnetic Modeling of SMM Setups with FE and FDTD Methods

Arif Gungor*[1], Malgorzata Celuch[2], Jasmin Smajic[1], Marzena Olszewska-Placha[2], Juerg Leuthold[1]

*: email: arifg@ethz.ch

[1]: Institute of Electromagnetic Fields (IEF), ETH Zurich

[2]: QWED Sp.z o.o

MMAMA

ETH zürich

Content

- Introduction
- Eigenvalue Analysis of Dielectric Resonator
  - FEM Analysis
  - FEM – FDTD Comparison Analysis
- Transient Analysis of SMM Tip
  - TD-FEM Formulation
  - FDTD – TDFEM Comparison
- Future Work
- Conclusion

Introduction

- What is SMM?

- Its use?
  - Micro- and nano- scale material characterization

- Different SMM Setups
  - Conductive fine tip
  - Dielectric resonator

- Why we need simulations of SMM Setups?

Eigenvalue Analysis of Dielectric Resonator

- Dielectric resonator
  - Axial symmetry
  - Anisotropic material: Sapphire
  - Whispering gallery modes

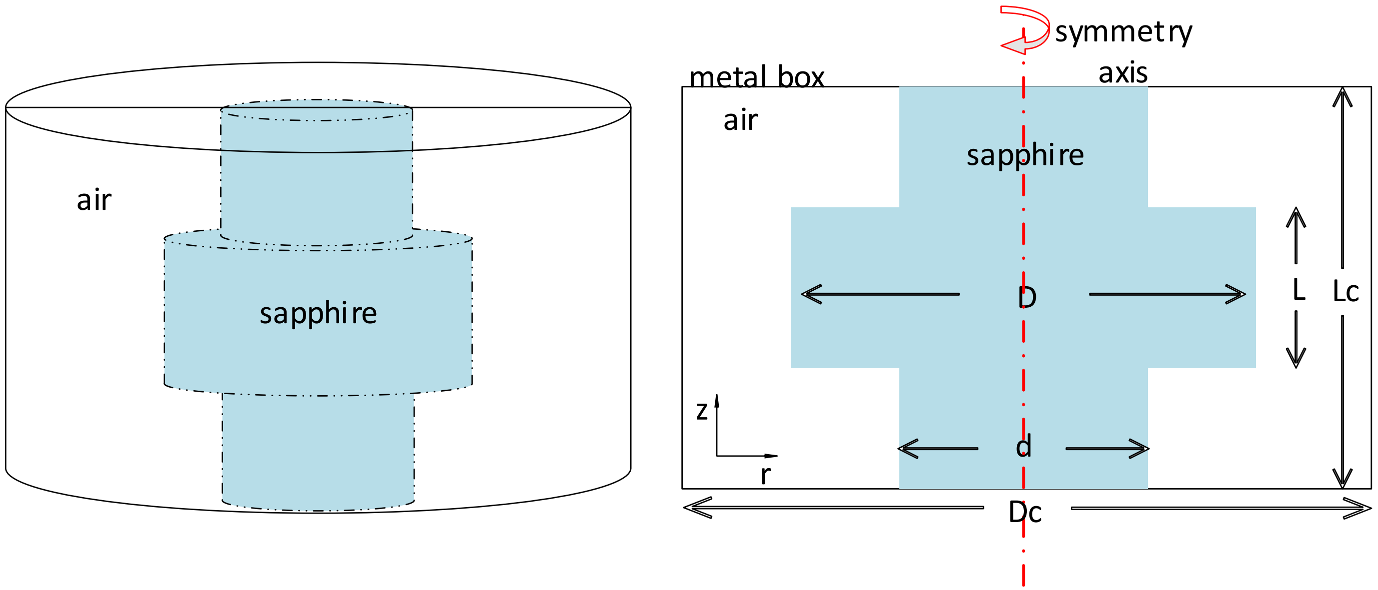

Eigenvalue Analysis of Dielectric Resonator

- Problem Definition

Ω_1: $\epsilon_{r\parallel} = 11.3532$, $\epsilon_{r\perp} = 9.2747$, $\mu_r = 1$, $\sigma = 0$ *(Sapphire)*

Ω_2: $\epsilon_{r\parallel} = 1$, $\epsilon_{r\perp} = 1$, $\mu_r = 1$, $\sigma = 0$ *(Air)*

$\nabla \times \frac{1}{\mu} \nabla \times \boldsymbol{E} - k_0^2 \boldsymbol{\varepsilon_r} \boldsymbol{E} = 0$ where $k_0^2 = \omega^2 \mu_0 \epsilon_0$ in $\Omega_1 \cup \Omega_2 = \Omega \subseteq R^2$

$\boldsymbol{n} \times \boldsymbol{E} = 0$ over $\partial\Omega_{\mathrm{PEC}} \subseteq R^1$ *(PEC condition)*

$\boldsymbol{n} \times \frac{1}{\mu} \nabla \times \boldsymbol{E} = 0$ over $\partial_4\Omega_1 \subseteq R^1$ *(axial symmetry condition)*

$\mathrm{m^{th}}$ azimuthal order, $\mathrm{e}^{-\mathrm{j}m\phi}$ dependence

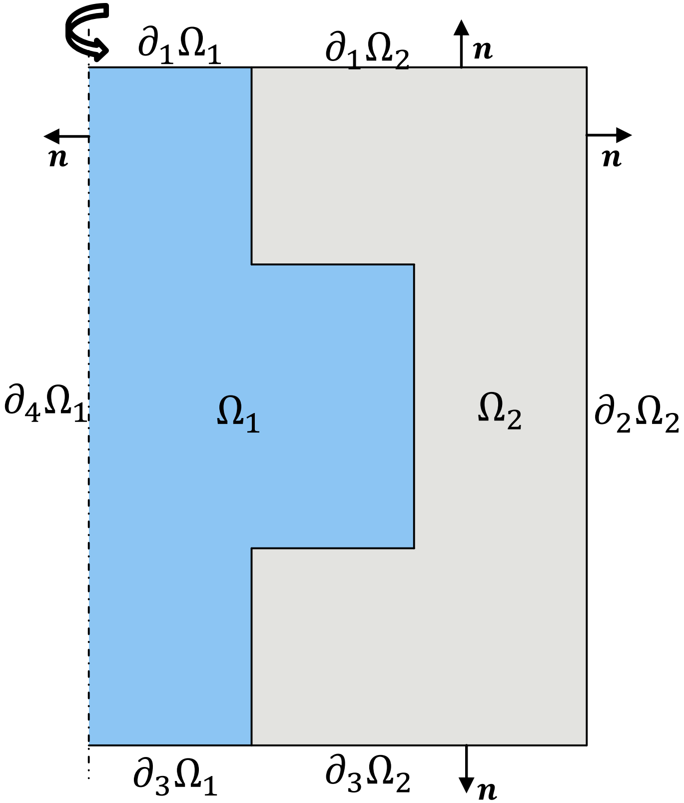

Sapphire Resonator

Eigenvalue Analysis of Dielectric Resonator

- Formulation
  - Angular dependence:

$$\boldsymbol{E} = E_\tau \boldsymbol{a_\tau} + E_\phi \boldsymbol{a_\phi} = \left[\boldsymbol{a_\tau} \sin(m\phi)\, e_\tau + \boldsymbol{a_\phi} \frac{\cos m\phi}{r} e_\phi\right]$$

  - Using Galerkin's method of weighted residuals, the weak form:

$$\iint \left\{\frac{1}{\mu_r}\left[r(\boldsymbol{\nabla_\tau} \times \boldsymbol{e_\tau^c}) \cdot (\boldsymbol{\nabla_\tau} \times \boldsymbol{e_\tau}) + \frac{m^2}{r}(\boldsymbol{e_\tau^c} \cdot \boldsymbol{e_\tau}) - \frac{m}{r}\left(\boldsymbol{e_\tau^c} \cdot \boldsymbol{\nabla_\tau} e_\phi + \boldsymbol{\nabla_\tau} e_\phi^c \cdot \boldsymbol{e_\tau}\right) + \frac{1}{r} \boldsymbol{\nabla_\tau} e_\phi^c \cdot \boldsymbol{\nabla_\tau} e_\phi\right]\right.$$

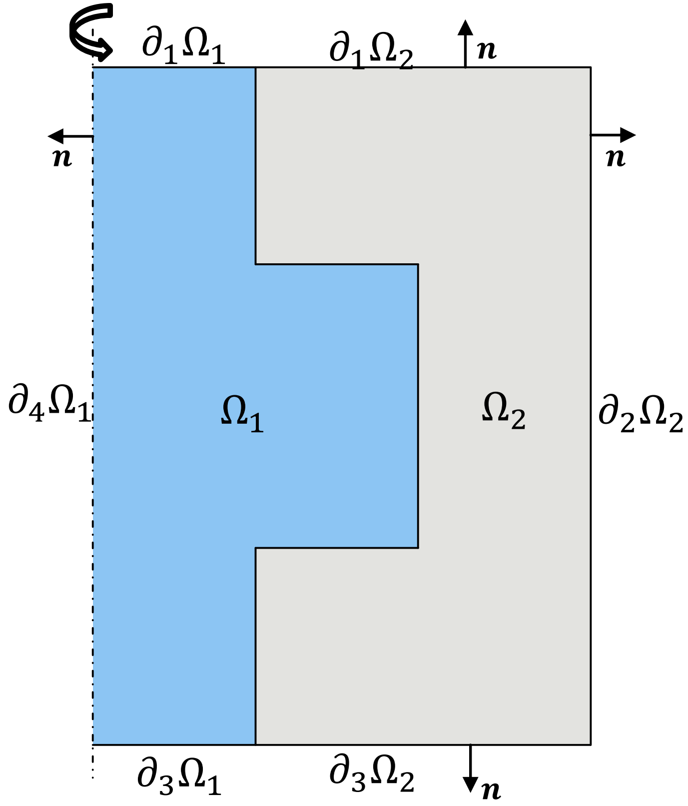

Sapphire Resonator

Eigenvalue Analysis of Dielectric Resonator

- FDTD Analysis and used methods
  - The Bodies-of-Revolution formulation [1] has been adapted
  - Three-step procedure comprising:
    - resonant frequency extraction of a coarse model with Prony method post-processing
    - refined resonance extraction on a refined mesh with Fourier transform
    - sine excitation for eigenmode pattern generation
  - Presently, signal co-processing has been enhanced to accelerate the process to ca. 5 min per resonant frequency

[1]: M. Celuch and W. Gwarek, "Accurate analysis of whispering gallery modes in dielectric resonators with BoR FDTD Method", 22nd International Microwave and Radar Conference MIKON 2018, 15-17 May 2018, Poznan, Poland.

Eigenvalue Analysis of Dielectric Resonator

- Results
  - 2 MHz absolute error

Mode-m	f_{C1} [GHz] comp.[2]	f_{E1} [GHz] exp. [2]	f_{FE} [GHz] FEM	Δf [MHz] $\lvert f_{FE} - f_{C1}\rvert$	Δf [MHz] $\lvert f_{FE} - f_{E1}\rvert$	f_{FD} [GHz] FDTD	Δf [MHz] $\lvert f_{FD} - f_{C1}\rvert$	Δf [MHz] $\lvert f_{FD} - f_{E1}\rvert$
N4-8	8.51317	8.51281	8.51298	0.19	0.17	8.51286	0.31	0.05
N4-9	9.19134	9.19115	9.19116	0.18	0.01	9.19122	0.12	0.07
N4-10	9.86408	9.86402	9.86385	0.23	0.17	9.86410	0.02	0.08
N4-11	10.52960	10.53188	10.53155	1.95	0.33	10.53190	2.30	0.02
N4-13	11.85206	11.85500	11.85393	1.87	1.07	11.85438	2.32	0.62
S1-10	8.21869	8.21760	8.21936	0.67	1.76	8.21751	1.18	0.09
S1-11	8.80633	8.80550	8.80674	0.41	1.24	8.80526	1.07	0.26
S1-12	8.39613	9.39560	9.396330	0.20	0.73	9.39500	1.13	0.60
S1-13	9.98764	9.98720	9.98761	0.03	0.41	9.98642	1.22	0.78
S1-14	10.58031	10.58000	10.580154	0.156	0.154	10.57933	0.98	0.67
S1-15	11.17389	11.17380	11.173635	0.255	0.165	11.17305	0.84	0.64

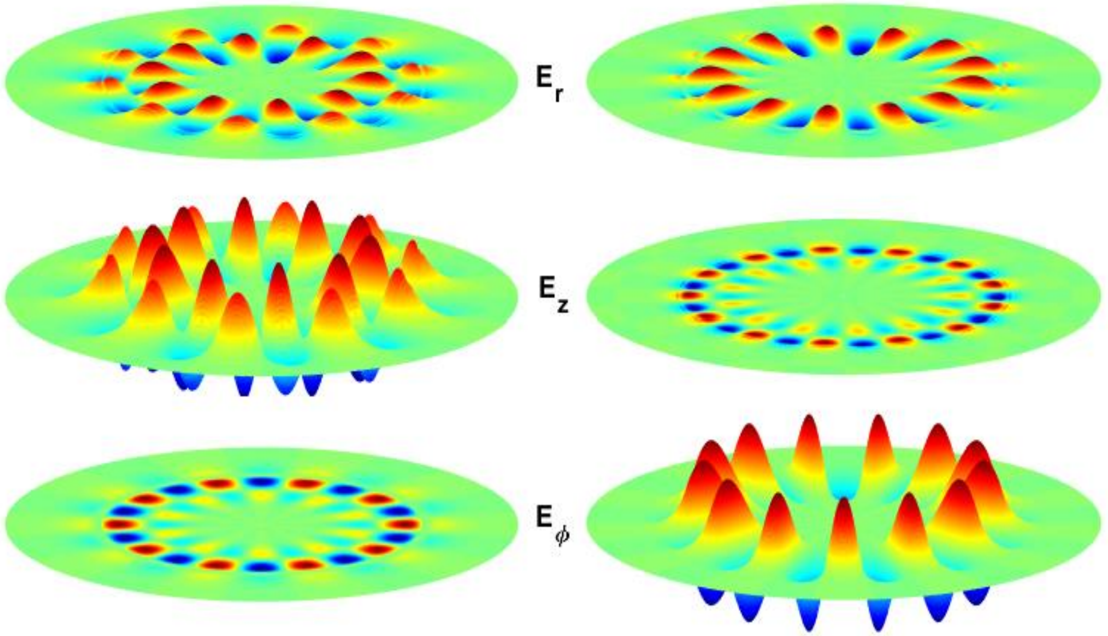

E-field profile (just above mid-plane) for two chosen modes: N4-10 (left) and S1-13 (right)

The modes are named after [2] to account for symmetry and angular dependence of the mode shape

[2]: Krupka, Jerzy, et al. "Use of whispering-gallery modes for complex permittivity determinations of ultra-low-loss dielectric materials." *IEEE Transactions on Microwave Theory and Techniques* 47.6 (1999): 752-759.

Transient Analysis of Conductive SMM Tip

- Conductive SMM Tip
  - Axial symmetry
  - Large aspect ratio (very fine tip and gap)
  - Applicable to advanced materials and device geometries

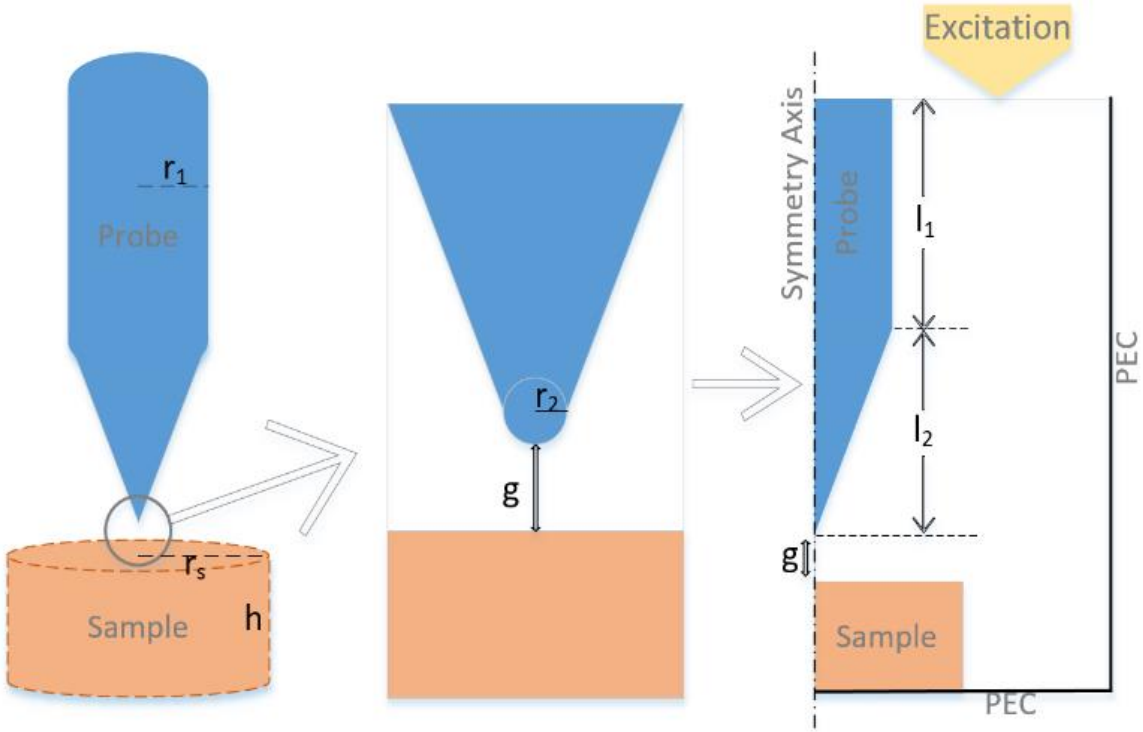

Transient Analysis of Conductive SMM Tip

- TD-FEM Analysis

$$\nabla \times \frac{1}{\mu}\nabla \times \boldsymbol{E} + \mu_0 \sigma \frac{\partial \boldsymbol{E}}{\partial t} + \mu_0 \varepsilon_0 \boldsymbol{\varepsilon_r} \frac{\partial^2 \boldsymbol{E}}{\partial t^2} = 0$$ in $\Omega_s \cup \Omega_a \subseteq R^2$

$$\boldsymbol{n} \times \boldsymbol{E} = 0$$ over $\partial_{PEC}\Omega \subseteq R^1$ *(PEC condition)*

$$\boldsymbol{n} \times \frac{1}{\mu}\nabla \times \boldsymbol{E} = 0$$ over $\partial_N \Omega \subseteq R^1$ *(Axial symmetry condition)*

$$\boldsymbol{n} \times \left(\frac{1}{\mu}\nabla \times \boldsymbol{E}\right) + \frac{\mu_0}{Z_{Port}}\boldsymbol{n} \times \left(\boldsymbol{n} \times \frac{\partial \boldsymbol{E}}{\partial t}\right) = \frac{-2\mu_0}{Z_{Port}}\boldsymbol{n} \times \left(\boldsymbol{n} \times \frac{\partial \boldsymbol{E_0}}{\partial t}\right)$$
over $\partial_{Port}\Omega \subseteq R^1$ *(Port Condition)*

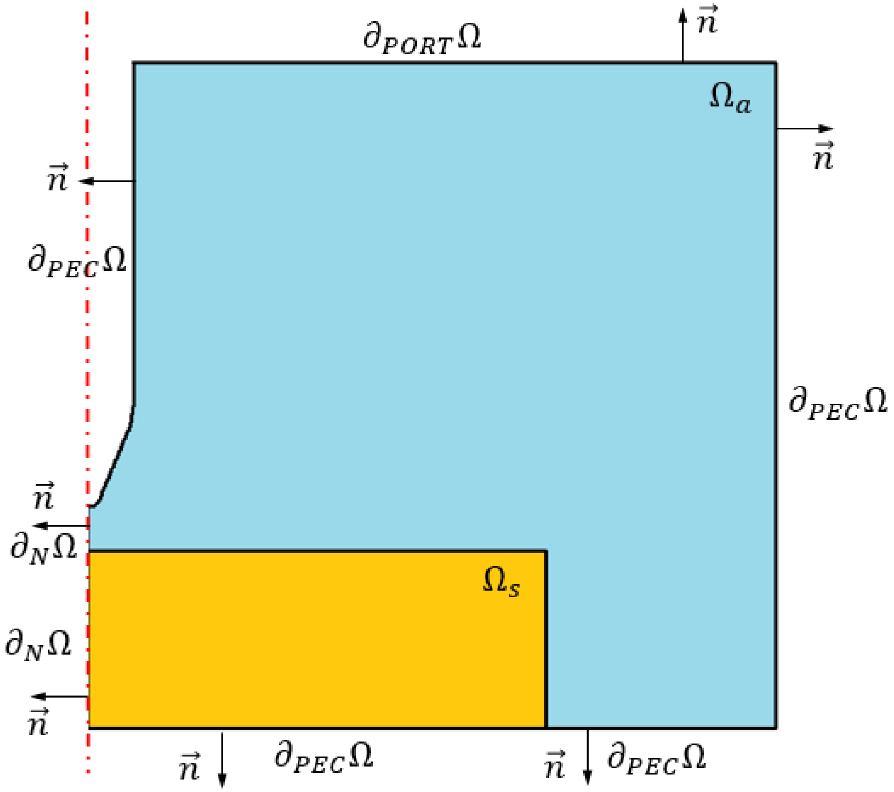

Conductive SMM Tip

Transient Analysis of Conductive SMM Tip

- FEM Discretization
  - Using Galerkin's method of weighted residuals, the weak form:

$$\iint \left\{ r\left(\frac{1}{\mu}\boldsymbol{\nabla}\times\boldsymbol{E}\right)\cdot(\boldsymbol{\nabla}\times\boldsymbol{E^c}) + \mu_0\sigma r\boldsymbol{E^c}\cdot\frac{\partial \boldsymbol{E}}{\partial t} + \mu_0\varepsilon_0\varepsilon r\boldsymbol{E^c}\cdot\frac{\partial^2 \boldsymbol{E}}{\partial t^2}\right\} dS + \frac{\mu_0}{Z_{Port}}\int r(\boldsymbol{n}\times\boldsymbol{E^c})\cdot\left(\boldsymbol{n}\times\frac{\partial \boldsymbol{E}}{\partial t}\right) dl = \frac{-2\mu_0}{Z_{Port}}\int r(\boldsymbol{n}\times\boldsymbol{E^c})\cdot\left(\boldsymbol{n}\times\right.$$

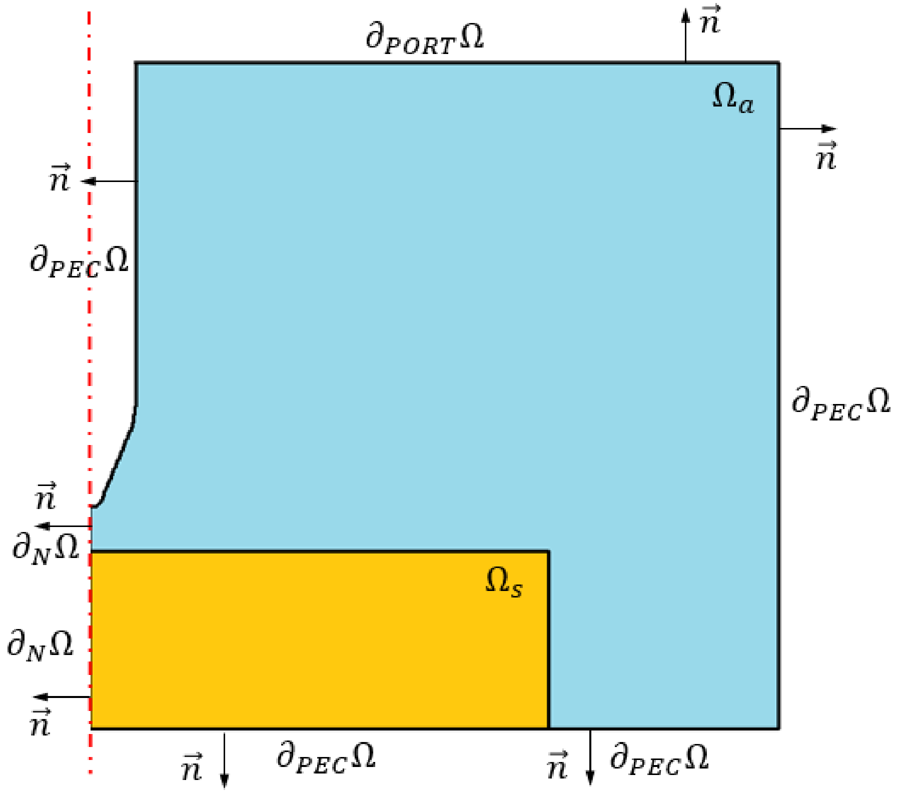

Conductive SMM Tip

Transient Analysis of Conductive SMM Tip

- FDTD Method and Analysis

  - TEM pulse excitation over 5-15 GHz band launched from the upper port
    - The excitation corresponds to a coax line

  - Fine space discretization near the fine tip and the air

  - FDTD analysis with a standard GPU code does not converge and the reflection coefficient results are corrupted with a numerical noise
    - A double-precision version of the FDTD code is implemented and executed on CPU

  - Simulations converge after several excitation periods
    - After a few seconds simulation on an average laptop computer
    - The required memory is within 1 MB

Transient Analysis of Conductive SMM Tip

- Results and Comparison

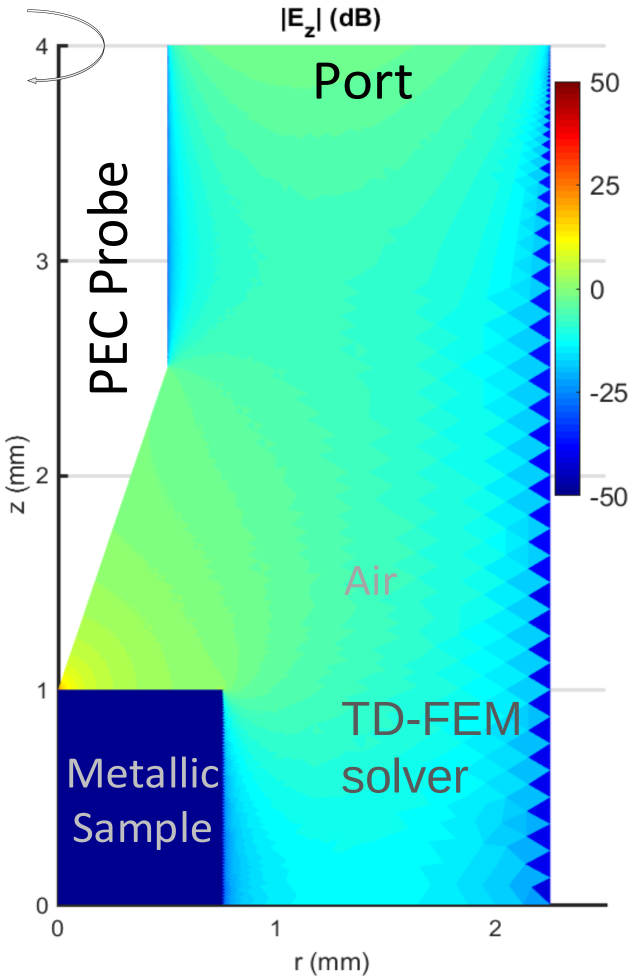

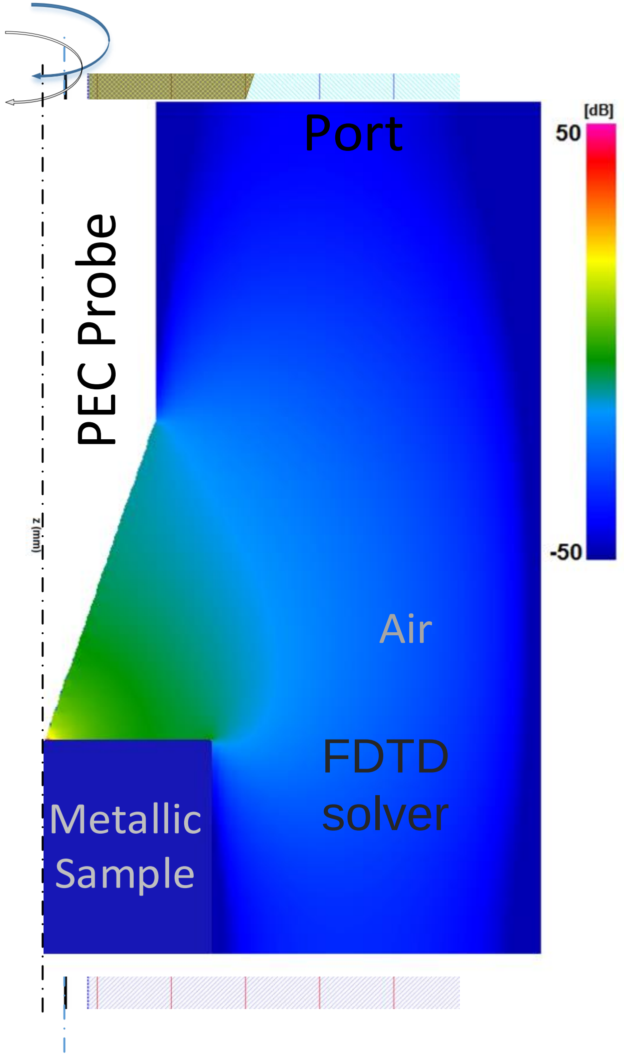

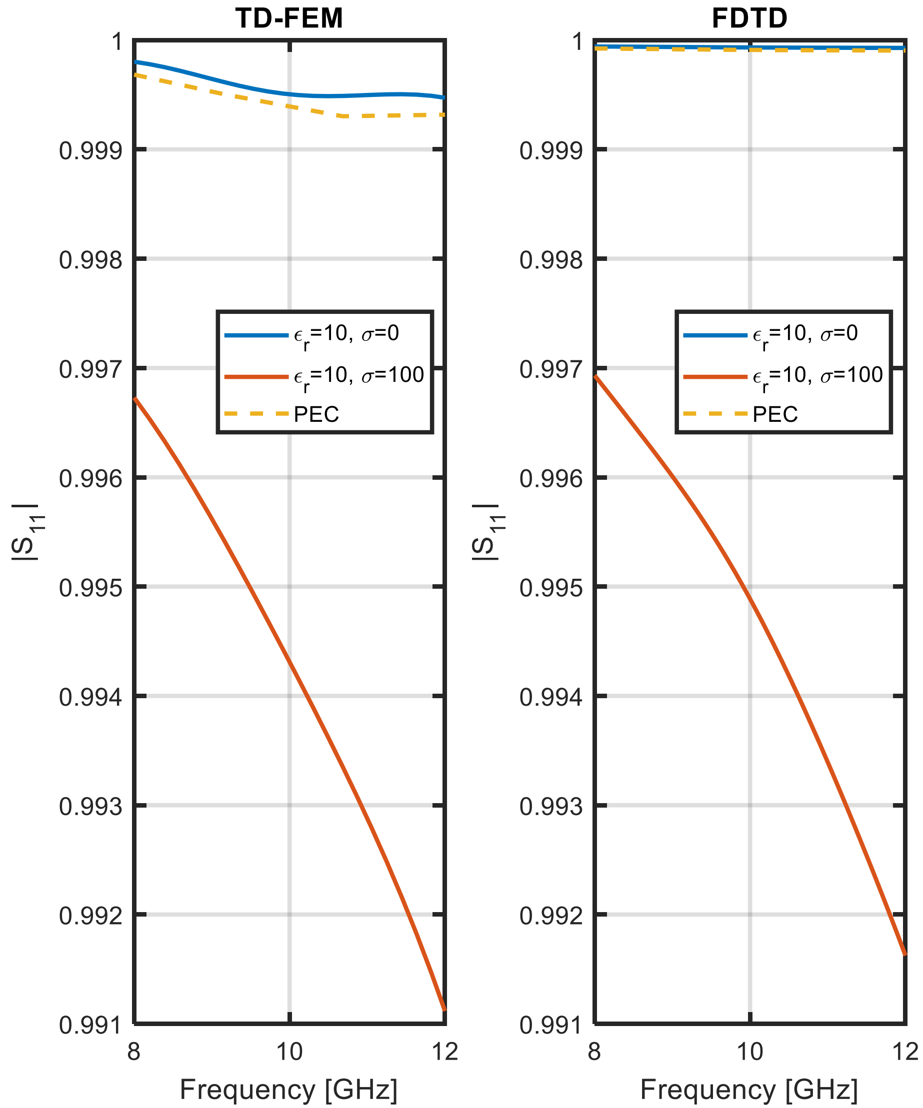

Future Work

- SMM on actual devices
  - Impedance and capacitance measurements
  - Preliminary results show a good agreement in capacitance
- Semiconductor samples
  - Local and changing conductivity due to charge movement with external field
- High (>100 GHz) frequency

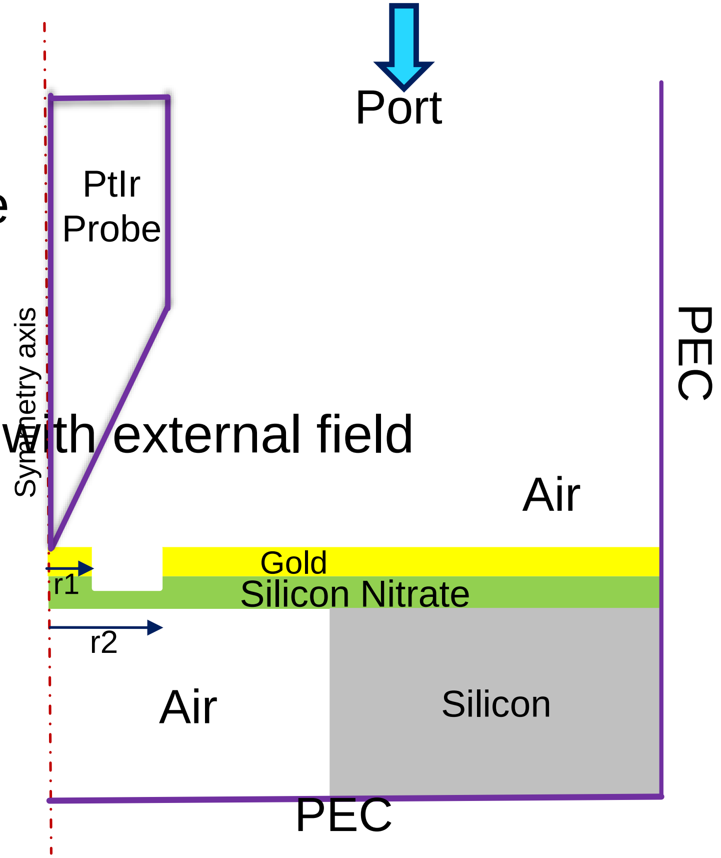

Conclusion

- Capabilities of FEM and FDTD solvers have been demonstrated for SMM setups based on
  - Dielectric resonator
    - Excellent agreement of resonant frequencies achieved by both the solvers
    - Frequency domain FEM is faster and more efficient
  - Metallic tip
    - Ability of simulating for very large aspect ratio geometry
    - Same behavior obtained for scattering parameters
    - Time domain FDTD is more effective than TD-FEM for transient problem
- Simulation of real life measurement conditions
- Applicable to advanced materials

Acknowledgement

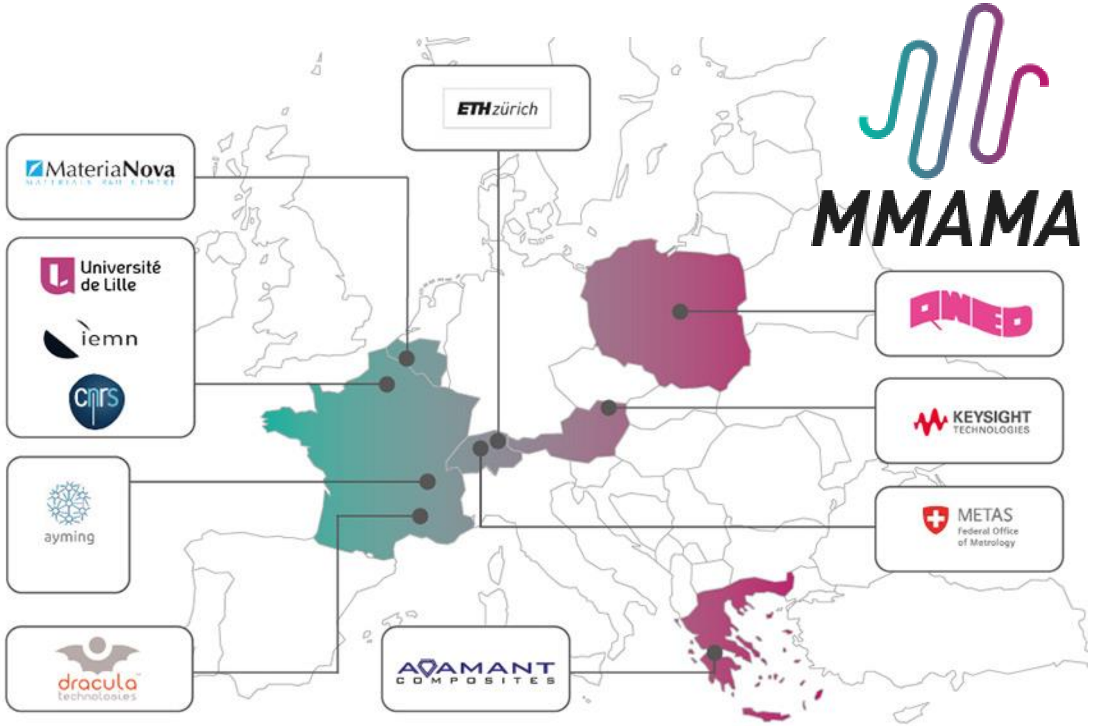

The work presented has received funding from the

European Union’s Horizon 2020

research and innovation programme (H2020-NMBP-07-2017) under grant agreement

MMAMA n°761036.

(website: www.mmama.eu)

Questions?